J. Fluid Mech. (1982), *vol.* 121, *pp.* 365–377
Printed in Great Britain

Estimates of the errors incurred in various asymptotic representations of wave packets

By M. GASTER

National Maritime Institute, Teddington, Middlesex, U.K.

(Received 16 March 1981)

An earlier paper (Gaster 1981) discussed different asymptotic representations of the isolated wave packet that evolved from an impulsive point excitation of a laminar boundary layer. Comparisons of the various asymptotic representations of the integral describing these packets were made on the basis of numerical evaluations of the various approximations together with the direct numerical solutions of the integral. Here the problem is pursued by analytical means, and error estimates are obtained for the different methods used.

1. Introduction

The process of transition from a laminar to a turbulent flow in a boundary layer is being studied experimentally at the National Maritime Institute. One of the experiments concerns the evolution of a wave packet initiated at a point on the surface of a flat plate. The resulting wave packet is three-dimensional, the amplitude of the disturbance is finite, and the motion evolves in a base boundary-layer flow that is increasing in thickness in the downstream direction. Interpretation of experimental data is further complicated by the fact that in the real flow there are various uncontrolled environmental factors that generate three-dimensional non-uniformities in the base flow and also introduce additional sources of unsteady disturbance. Before embarking on a full interpretation of the experimental observations it is desirable to try and break down the solution into individual tractable sub-problems that can be tackled analytically. In so doing it is inevitable that the sub-problems will appear to be somewhat contrived, but this need not prevent the exercise from being valuable. Here we are concerned with asymptotic descriptions of a two-dimensional wave packet. In order to clarify certain issues that have arisen in defining appropriate expansions we consider an idealized and quite artificial flow – a parallel boundary layer. The analysis discusses the asymptotic expansion of a pulse-excited wave packet propagating in this parallel flow. The simplification enables precise expansions to be derived, and provides estimates of the errors incurred in their use. It is intended to apply the results of this work to physically more realistic problems involving boundary-layer growth and three-dimensionality of the packet (see Craik 1981).

The following discussion is concerned with the linear stability of a parallel mean shear layer perturbed by a stream function in the form of a travelling wave

$$\phi(y) \exp i(\alpha x - \omega t),$$

where $\phi(y)$ defines the internal structure of the disturbance through a stream function, α is the wavenumber and ω the frequency parameter. It is generally found that instabilities can occur at sufficiently large Reynolds numbers. Such instabilities are defined by a dispersion relation, $\omega = F(\alpha)$ say, that links the frequency and the wavenumber of possible eigenmodes. Instabilities in the form of exponentially growing waves (increasing in amplitude with x when $\alpha_i < 0$, or with t when $\omega_i > 0$) often arise over a range of real frequencies or wavenumbers. A wavemaker at some fixed location, executing simple harmonic motion at a frequency ω_0 that lies within this band, will generate a propagating wavetrain of the form

$$\psi(x,y,t) = \mathscr{R}\{\phi(y,\alpha(\omega_0),\omega_0)\,e^{i(\alpha(\omega_0)\,x-\omega_0\,t)}\}, \tag{1}$$

where $\alpha(\omega_0)$ is defined by the appropriate dispersion relation, and where $\mathscr{R}\{\ \}$ denotes the real part of $\{\ \}$.

Excitation in the form of a discrete pressure pulse acting at a point on the boundary results in a disturbance described by an integral of the above travelling waves over all wavenumbers:

$$\psi(x,y,t) = \mathscr{R}\{\textstyle\int\phi(y,\alpha,\omega(\alpha))\,e^{i(\alpha x-\omega(\alpha)\,t)}\,d\alpha\}. \tag{2}$$

The evaluation of (2), at any given value of y, can of course be obtained at every point on the (x,t)-plane by direct numerical summation, but this rather cumbersome approach does not lead to helpful mathematical descriptions of the flow. It turns out that in cases of real practical interest we are concerned with the evaluation of (2) at relatively large values of x or t, where it is appropriate to use asymptotic approximations.

At large x or t the major contribution to the integral in (2) arises from the exponential term, and it will suffice for the purpose of the present discussion to concentrate on the evaluation of the simpler integral

$$I_\alpha = \int \exp i(\alpha x - \omega(\alpha)\,t)\,d\alpha. \tag{3}$$

In Gaster (1981, hereinafter referred to as I) approximations to the above integral were discussed for the dispersion appropriate to the parallel-flow approximation to the flat-plate boundary layer at a Reynolds number R of 1000. In this problem the modes are well separated, and it is appropriate, at large x or t, to consider only that contribution arising from the dominant travelling-wave mode, and to neglect the influence of higher modes or of any continuous spectrum. It has been shown (Gaster 1978*a*) that a good representation of the dispersion of the dominant mode for such a flow is given by the power series

$$\frac{\omega}{\alpha} = \sum_{n=0}^{N}\sum_{m=0}^{M} A_{nm}(\alpha R-(\alpha R)_0)^n\,(\alpha^2-\alpha_0^2)^m. \tag{4}$$

Over the parameter range of interest in this problem the series either converged to sufficient accuracy, or could be 'helped' to do so by the use of a nonlinear Shanks transformation on the partial sums.

Three asymptotic representations of (3) for large t were considered in I. The resulting expressions were evaluated numerically and then compared with numerical summations, which will here be called 'exact' solutions. Whereas two of these approximations provided solutions that approached the exact result as $t\to\infty$, albeit at different rates, the third expansion generated wave-packet shapes that were far removed from those derived by summation, even at the largest values of x considered. From the computations it was not at all clear whether this type of approximation was in fact a true asymptote to (3). The particular expansion in question arose from the so-called 'real-axis approximation' (RAA), which has sometimes been used to describe linear wave patterns in cases of weak instability (Gaster 1968*a*; Landahl 1972).

In conservative wave systems, where the dispersion is purely real, the concept of wave groups propagating away from a source along the group vector is well founded. The Fourier components of any initial disturbance will then propagate away from the source with their appropriate group velocities, and it is a relatively straightforward matter to evaluate the resultant motion. Fluid-dynamic stability problems, where a band of waves may be weakly amplified whilst others are damped, exhibit dispersions that are not wholly real. It is nevertheless tempting to use this simple kinematic solution to describe the evolution of instabilities even though the dispersion relations contain some relatively weak imaginary terms. This has been attempted by making the assumption that the real part of the dispersion controls the direction and speed of propagation of different wave groups, while the weak imaginary part controls the actual magnitudes of the waves at the different locations. Account for dissipation, or for any positive energy transfer to the waves through an instability mechanism, is then made through a suitable weighting applied to the amplitudes given by the ray theory. This idea has been shown (Stewartson 1973; Gaster 1978*b*) to be applicable to pulse-excited wave packets only in those cases where a certain dispersion parameter is very small – a condition not satisfied by the instability waves that occur in the boundary layer on a flat plate. This limitation of the RAA has been the source of some controversy in recent years. It turns out that the most-unstable waves are quite properly represented by the approach, and one might well expect (and this is the basis for the method) that at least the central region of the packet surrounding the most-amplified ray would also be modelled reasonably closely. But in I the real-axis approximation did not appear to asymptote to the proper limiting solution for very large x or t. Since this problem was not properly resolved by the numerical computations, it seemed worth examining the asymptotic behaviour of the various approximations in greater depth.

2. Asymptotic approximations

2.1. *Steepest descent*

The integral in (3) can be expressed as an asymptotic series most effectively by the method of steepest descent, where the exponent is expanded about a saddle-point in the complex α-plane. The series is given by

$$I_\alpha \sim \left[\frac{2\pi}{i\dfrac{\partial^2\omega}{\partial\alpha^2}(\alpha^*)\,t}\right]^{\frac{1}{2}} e^{i(\alpha^* x/t-\omega(\alpha^*))t}\left[1+\frac{A_1(\alpha^*)}{t}+\frac{A_2(\alpha^*)}{t^2}+\dots\right], \tag{5}$$

where for each ray, defined by x/t, a point α^* is chosen such that

$$\frac{\partial}{\partial\alpha}\left(\alpha\frac{x}{t}-\omega(\alpha)\right)=0 \quad \text{at } \alpha^*. \tag{6}$$

The steepest-descent expansion can be carried out on (3) either by integrating over the α-plane to give (5), or by changing the variable and the integrating with respect to ω in the form

$$I_\omega = \int \frac{\partial\alpha(\omega)}{\partial\omega}\, e^{i(\alpha(\omega)-\omega t/x)\,x}\, d\omega. \tag{7}$$

When the integration is carried out in the ω-plane it turns out to be convenient to treat x as the large parameter of the expansion, and hence to derive the series in inverse powers of x:

$$I_\omega \sim \left[\frac{2\pi}{-i\dfrac{\partial^2\alpha}{\partial\omega^2}(\omega^*)\,x}\right]^{\frac{1}{2}} \frac{\partial\alpha}{\partial\omega}(\omega^*)\, e^{i(\alpha(\omega^*)-\omega^* t/x)\,x}\left[1+\frac{B_1}{x}+\frac{B_2}{x^2}+\ldots\right]. \tag{8}$$

To leading order, at least, the above expression is identical with (5), since for real x/t we have

$$x/t = \frac{\partial\omega_r}{\partial\alpha}(\alpha^*) = 1\bigg/\frac{\partial\alpha_r}{\partial\omega}(\omega^*),$$

where α^* is identical with $\alpha(\omega^*)$, and

$$\frac{\partial^2\alpha}{\partial\omega^2}(\omega^*) \equiv -\frac{\partial^2\omega}{\partial\alpha^2}(\alpha^*)\bigg/\left[\frac{\partial\omega}{\partial\alpha}(\alpha^*)\right]^3. \tag{9}$$

The ray defined by the value of x/t for the most-amplified waves will, however, be different in the two frames of reference. In the temporal sense the most rapidly growing disturbances occur along the ray defined by $\alpha_i^* = 0$ (Gaster 1968*b*), while in the spatial case maximum growth takes place where $\omega_i^* = 0$. The saddle points defined by these two conditions will have different projections in physical space, which are linked to different values of the group velocity. The real rays along which the growth rate is at a maximum will therefore not be coincident in the two frames of reference, and this has repercussions in the approximate solutions that rely on expansions about the most-unstable ray. Different approximations then arise in the two reference frames.

The numerical evaluation of (5) requires either that the dispersion be known explicitly, or that (6) can be satisfied and all the necessary derivatives defining the As found numerically for any given x/t. In I the leading term was evaluated for a range of values of x and t, and the resulting wave-packet shapes were compared with those obtained from the direct numerical summation – the 'exact' solution. In fact at large x or t the agreement between these two sets of results was found to be extremely good. The complex coefficients A_1, A_2 and A_3 have now also been computed from the expressions given in appendix A for the dominant ray, where $x/t = 0{\cdot}424$:

$$A_1 = (5{\cdot}036,\ 0{\cdot}8873),\quad A_2 = (79{\cdot}85,\ 705{\cdot}0),\quad A_3 = (1{\cdot}393,\ 1{\cdot}365)\times 10^5. \tag{10}$$

For neighbouring rays values very similar to the above were obtained, but for rays well away from the centre of the packet the series representation of the dispersion failed to converge well enough to give accurate values of the higher derivatives in the expression for the As. The difficulty arose purely because the dispersion series was based on an expansion about a real value of the wavenumber. This provided better convergence at the centre of the wave packet than at the edges, but there is no reason to expect the coefficients A_1, A_2, etc., to behave in other than a smooth manner with x/t. The error incurred in truncating the asymptotic series, which will be proportional to the leading term on that ray, is likely to be of similar magnitude over the whole of a packet. In retrospect, then, it is not at all surprising that such excellent agreement between the leading term of the steepest-descent expansion and the exact solution was achieved in I, as the predicted error, based on A_1, turns out to be of order 0·25 % at an x of 800, and is still only 2 % at a distance of 100 displacement thicknesses from the source.

2.2. *Gaussian*

The 'Gaussian' approximation to the integral is obtained by truncating the expansion of the exponent in (4) to second degree and integrating the resulting expression in closed form. The dispersion relation can be expanded about any convenient mode – but it is usual to choose the one associated with the rays that form the centre of the packet. At large values of t this will be close to the eigenmode with α_i^* equal to zero. It should be noted that at finite values of x the square-root term in the denominator will have the effect of moving the position of the maximum of the wave packet envelope away from that given by the limiting ray for the most amplified mode. But here we are concerned with the asymptotic behaviour, and it will suffice to expand about the point $\alpha^{\#}$, where $(\partial\omega/\partial\alpha)(\alpha^{\#})$ is real.

Equation (3) can then be integrated completely with the result

$$I_\alpha \sim \left[\frac{2\pi}{i\dfrac{\partial^2\omega}{\partial\alpha^2}(\alpha^{\#})\,t}\right]^{\frac{1}{2}} \exp i\left\{\left(\alpha^{\#}\frac{x}{t}-\omega(\alpha^{\#})\right)+\left(\frac{x}{t}-\frac{\partial\omega}{\partial\alpha}(\alpha^{\#})\right)^2\Big/2\frac{\partial^2\omega}{\partial\alpha^2}(\alpha^{\#})\right\}t. \tag{11}$$

For the ray $x/t = (\partial\omega_r/\partial\alpha)(\alpha^{\#})$ the above result is identical with that given by the steepest-descent expansion, and for neighbouring rays defined by $x/t = \epsilon + V_g$, where V_g is the group velocity of the dominant ray, the right-hand side of (11) becomes

$$\left[\frac{2\pi}{i\dfrac{\partial^2\omega}{\partial\alpha^2}(\alpha^{\#})\,t}\right]^{\frac{1}{2}} \exp i\left\{\left(\alpha^{\#}(V_g+\epsilon)-\omega(\alpha^{\#})\right)+\epsilon^2\Big/2\frac{\partial^2\omega}{\partial\alpha^2}(\alpha^{\#})\right\}t, \tag{12}$$

for small values of ϵ.

Since the leading term of the steepest-descent asymptotic series provides such a good estimate of the solution (with error of order $|A_1|/t$), this result can be used to assess the accuracy of other less-precise approximations, at least to that order. The leading term of the steepest descent expansion for small ϵ (see appendix B) is

$$-\epsilon^3\frac{\partial^3\omega}{\partial\alpha^3}(\alpha^{\#})\Big/6\left[\frac{\partial^2\omega}{\partial\alpha^2}(\alpha^{\#})\right]^3+\ldots, \tag{13}$$

showing the Gaussian result to be in error by a cubic term in the exponent of magnitude $-i\epsilon^3K_1t$, where $K_1 = (0{\cdot}2989,\ -1{\cdot}348)$.

2.3. *The real-axis approximation*

In this approximation the dispersion is treated as if it were real in so far as the propagation of the different wavenumber groups is concerned, whilst the imaginary component determines the actual magnitude of the waves. Each point, designated +, on the real α-axis, maps onto the (x, t)-plane through the relation

$$\frac{x}{t} = \frac{\partial\omega_r}{\partial\alpha}(\alpha^+),$$

and provides the solution

$$\left[\frac{2\pi}{i\dfrac{\partial^2\omega_r}{\partial\alpha^2}(\alpha^+)\,t}\right]^{\frac{1}{2}} \exp i\left\{\alpha^+\frac{x}{t}-\omega(\alpha^+)\right\}t. \tag{14}$$

The above expression, which is equal to the asymptotic result for the most-amplified ray where $\omega_i(\alpha^\#) = 0$, can be developed in a series expansion in ϵ (see appendix C) by the same procedure that was used in the discussion of the Gaussian approximation. Expression (14) then becomes

$$\left[\frac{2\pi}{i\frac{\partial^2\omega}{\partial\alpha^2}(\alpha^\#)\,t}\right]^{\frac{1}{2}} \exp i\left\{\left(\alpha^\#\frac{x}{t} - \omega(\alpha^\#)\right) + \epsilon^2 K_2 + \epsilon^3 K_3 + \ldots\right\} t \tag{15}$$

for small ϵ, where

$$K_2 = \frac{\omega_r'' - i\omega_i''}{2(\omega_r'')^2},$$

$$K_3 = \frac{1}{6(\omega_r'')^4}[3\omega_r'''\omega'' - 3\omega_r'''\omega_r'' - \omega'''\omega_r''].$$

This result may be compared directly with the expansion derived for the leading term of the steepest-descent result when this is also written out in terms of ϵ. It is apparent that the RAA, as defined by (14), is in error at the term involving ϵ^2 in the exponent, of magnitude (2·879, 13·25).

In a previous attempt (Gaster 1978*b*) to draw attention to the possible pitfalls of using the RAA, the steepest-descent result was linked to parameters on the real axis for situations when the saddle point lies close to the real axis. This produced the expansion

$$\left[\frac{2\pi}{i\frac{\partial^2\omega}{\partial\alpha^2}(\alpha^\#)\,t}\right] \exp i\left\{\left(\alpha^+\frac{x}{t} - \omega(\alpha^+)\right) - \left(\frac{\partial\omega_i}{\partial\alpha}(\alpha^+)\right)^2 \Big/ 2\frac{\partial^2\omega}{\partial\alpha^2}(\alpha^+) + \ldots\right\} t, \tag{16}$$

which reduced to the simpler form (14) if

$$\left|\left(\frac{\partial\omega_i}{\partial\alpha}(\alpha^+)\right)^2 \Big/ \frac{\partial^2\omega}{\partial\alpha^2}(\alpha^+)\right| \ll |\omega(\alpha^+)|, \tag{17}$$

a condition not realized in the instability waves that occur in the flat-plate boundary layer, except at the centre of the packet where $(\partial\omega_i/\partial\alpha)(\alpha^+)$ is identically zero. It is worth noting that the exponent of the extended form of the RAA can be written (see appendix C) as

$$i\left\{\left(\alpha^\#\frac{x}{t} - w(\alpha^\#)\right) + \epsilon^2 \Big/ 2\frac{\partial^2\omega}{\partial\alpha^2}(\alpha^\#) + K_4\epsilon^3 + \ldots\right\} t, \tag{18}$$

which is only in errror at the cube of ϵ, where K_4 is

$$\frac{1}{2(\omega_r'')^3}\left[-\omega_r''' + \frac{\omega_r'''\omega''}{\omega_r''} - \tfrac{1}{3}\omega''' + \frac{(\omega_i'')^2}{\omega''}\left(-\frac{\omega'''}{\omega''} + \frac{\omega_i'''}{\omega_i''} - \frac{\omega_r'''}{\omega_r''}\right)\right] \tag{19}$$

and has a numerical value equal to (131·9, 27·8).

3. Discussion

The integral formulation of the wave-packet solution is ideally suited to evaluation by the method of steepest descent. This technique produces an asymptotic-series solution along any given ray x/t in terms of t. From the first few terms of this series, for the specific case of instability waves on a flat plate, the approximation is very good indeed for values of x occurring in cases of practical interest. In fact, the leading term by itself is accurate to roughly 0·25 % at a distance of 800 boundary-layer displacement thicknesses from the source, the farthest distance for which numerical comparisons were made in I. The inclusion of higher terms would effectively enable a precision of a few parts per 100 000 to be obtained! At even quite short distances from the source, where asymptotic techniques seem hardly applicable, the leading term provides approximations that are accurate to a few per cent. The numerical results presented in I are entirely consistent with these estimates.

The Gaussian approximation has been compared with the leading term of the steepest-descent asymptote in the neighbourhood of the ray defining the most-amplified waves. For the particular dispersion under discussion the ratio of this solution to that of the steepest-descent approximation is

$$e^{iK_1 \epsilon^3 t}, \tag{20}$$

where $K_1 = (0{\cdot}2989,\ -1{\cdot}348)$. Therefore for a constant value of ϵ (of appropriate sign) the error will increase exponentially with t, i.e. in these co-ordinates the Gaussian approximation does not asymptote to the true solution. However, since the width of the wave packet effectively decreases in terms of ϵ with increasing t, it is appropriate to use a similarity scaling $\xi = \epsilon^2 t$ that takes account of this factor. Then, for a given ξ, the ratio of the Gaussian approximation to the steepest-descent term will behave like

$$e^{K/t^{\frac{1}{2}}}, \tag{21}$$

and this can be made as small as desired by taking t large enough. To assess the magnitude of this error it is convenient to consider the points ϵ_0, where the amplitude of the wave-packet envelope is one-half that at the peak. For the Gaussian solution

$$\epsilon_0 = \pm \left[\frac{\log \frac{1}{2}}{-Kt}\right]^{\frac{1}{2}}, \tag{22}$$

where $$K = 0{\cdot}5971, \quad \epsilon_0 = \pm\, 1{\cdot}078 t^{-\frac{1}{2}}.$$

The cubic term in (13) gives rise to an error at ϵ_0 of $\exp\{\pm(1{\cdot}689 + 0{\cdot}374i)\, t^{\frac{1}{2}}\}$, which at 800 displacement thicknesses downstream (where $t = 800/0{\cdot}424$) is 4 % in amplitude.

The real-axis approximation provides a solution that can be compared with the leading term of the steepest-descent series to give the ratio

$$e^{i(K_2 - K_0)\epsilon^2 t}, \tag{23}$$

where $$K_2 = \frac{\omega_r'' - i\omega_i''}{2(\omega_r'')^2}, \tag{24}$$

$$K_0 = \frac{1}{2\omega''}. \tag{25}$$

The real part of K_2 must always be greater than the real part of K_0, and in the present example the real part of the resultant difference in the exponent is $-\epsilon^2 t \times 1{\cdot}325$. Therefore the RAA solution does not asymptote to the correct solution as $t \to \infty$ when keeing x constant. It turns out from these values that the width of the packet as defined by the half-amplitude points is only one-fifth that given by the Gaussian solution. However, the extended form of expansion given by (15) will behave like the Gaussian solution in that it does asymptote correctly, but in this case the coefficient of the cubic error term is very large and consequently the limit is approached more slowly than for the Gaussian solution. For example t has to be greater than 12×10^6 for the error to be less than 1 %.

One of the referees has pointed out that this behaviour is to be expected for the pulse-driven wave packet, because in that case rays are being traced over distances very much greater than the length of the original packet, and this leads to unacceptable cumulative errors. He implies that the evolution of a given packet containing many cycles could nevertheless be traced for distances up to that of the length of the packet. Although this may well be true for certain types of complex dispersion, it does not appear to be a useful approach for the specific case discussed here. In the boundary-layer example it turns out that the dispersive effects given by the real-axis rays are, in magnitude, only about one-fifth the correct value, and that group velocity $\partial\omega_r/\partial\alpha$ has a maximum value ($\partial^2\omega_r/\partial\alpha^2$ is zero at a point on the real axis). Thus although the central region of the packet may be adequately represented for some distance downstream, the leading and trailing edges will contain errors that increase with distance.

4. Conclusions

The analysis presented here provides a useful guide to the accuracy of various asymptotic representations of a point-excited wave packet in a 'parallel boundary layer'. Real boundary layers grow with distance downstream, and this can be expected to add considerably to the complexity of the problem. Nevertheless, it is helpful to have solutions to the simpler problem before constructing more-realistic models to represent the experiments. The method of steepest descent has been used to evaluate the asymptotic-series solution describing a wave packet generated impulsively at a point. Previously, only the leading term had been computed and, although this was shown to compare closely with the numerical summation of the integral describing the solution, no error estimates were made. Here three terms of the series have been evaluated. They show that, at distances from the source of practical interest in the context of transition studies, very great accuracy can be achieved. For most purposes it would only be necessary to evaluate the leading term to achieve solutions within 0·25 % of the exact result.

The Gaussian approximation has also been compared with the leading term of the steepest-descent asymptote. This form of approximation arises quite naturally as the leading term of a multiple-scale approach, but error estimates are not generally made. Such estimates have been obtained in the neighbourhood of the envelope maximum by comparing the different expansions of the solutions for small ϵ. It turns out that the extent of a packet, in terms of x/t, decreases with t. In appropriate variables that incorporate this scaling, the Gaussian solution approaches the steepest-descent asymptote like $\exp(Kt^{-\frac{1}{4}})$. At very large distances from the source a reasonably good representation of a wave packet is thus provided, but at typical distances that arise in experiment the errors can be significant. At a distance of 800 displacement thicknesses from the source, for example, the cubic term in the exponent leads to an error of 4% in the amplitude at ϵ_0, the position where the envelope has half the peak amplitude.

Finally, a similar analysis was carried out on the real-axis approximation. In this

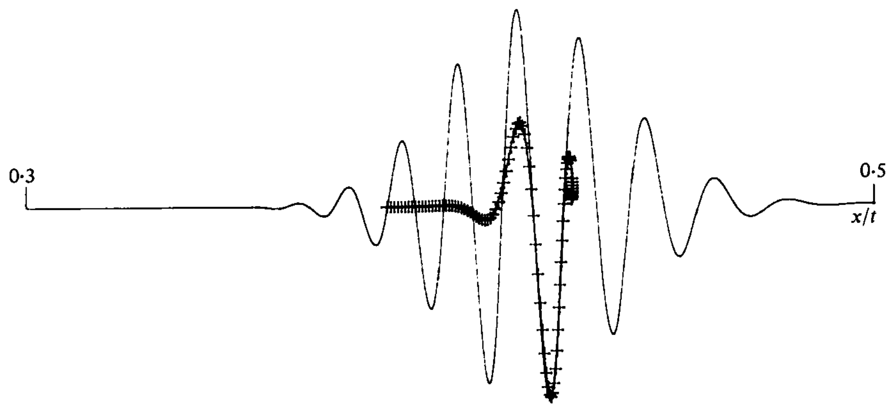

FIGURE 1. Comparison of wave packets calculated from Gaussian model (12) (———) and real-axis approximation (14) (+ + + +).

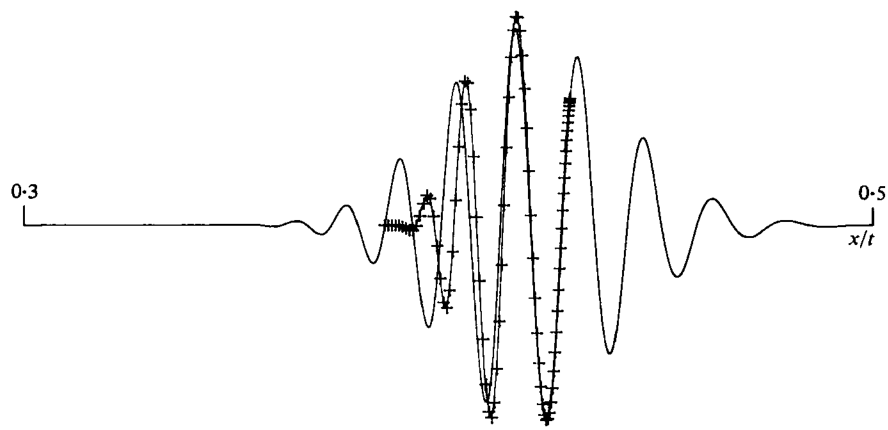

FIGURE 2. Comparison of wave packets calculated from Gaussian model (12) (———) and modified real-axis approximation (10) (+ + + +).

case the approximation was shown to provide a wave packet that was always of narrower extent in x/t than the true wave packet, even in the limit as $t \to \infty$. In fact the approximation did not asymptote to the true solution at all. The addition of another term to the approximation was, however, shown to provide a proper asymptote, with an error term of the same form as the Gaussian solution, but of much greater numerical value. In fact, at $x = 800$ the error at the half-amplitude positions is $e^{\pm 0\cdot 798}$. The predicted behaviour is illustrated in figures 1 and 2, which compare the Gaussian wave-packet approximation at $x = 800$ with the two forms of the real-axis approximation. Clearly, both are unacceptable approximations at this distance from the source but, whereas the simple level of approximation (14) does not tend to the Gaussian shape, the second solution containing the extra term does, albeit extremely slowly, as $t \to \infty$.

In general the method of steepest descent is to be preferred, as it provides approximations of the highest accuracy. There are cases, however, when it is desirable to be

n	Derivatives $\partial^n\omega/\partial\alpha^n(\alpha^{\#})$ Real part	Imaginary part
0	0·094892	0·003142
1	0·424083	0·0
2	0·173676	−0·799632
3	−2·96314	−3·44016
4	−15·3797	9·60055
5	−149·565	−481·387
6	−7294·26	5119·31
7	−107613	−172050

TABLE 1

able to have a simple closed-form expression for the wave packet. Provided that the distance from the source point is large enough and the highest precision is not required, the Gaussian approximation may then be of use. Finally, it is concluded that the use of the real-axis approximation, even with the additional term, is quite inappropriate in the context of wave-packet evolution in boundary layers.

This programme is supported by the U.S. Air Force (AFOSR Grant-80-0272); The Ministry of Defence, Royal Aircraft Establishment, Farnborough; The Admiralty Underwater Weapons Establishment, Portland; and the Department of Industry.

Appendix A. Higher-order terms of the steepest-descent expansion

For the parallel-flow approximation to the flat-plate boundary layer it has been found that the dominant instability waves can be represented by the series dispersion relation

$$\frac{\omega}{\alpha} = \sum_{n=0}^{N} \sum_{m=0}^{M} A_{nm}(\alpha R - (\alpha R)_0)^n (\alpha^2 - \alpha_0^2)^m. \tag{A 1}$$

The technique used to sum the above series, which may not always appear to converge very well, by the application of a nonlinear Shanks' transformation, has been discussed by Gaster (1978*a*). For the specific case chosen as an example for the calculations presented in I and in this paper, the Reynolds number is 1000 (based on the displacement thickness), and it is found that the most-unstable temporal mode

$$((\partial\omega_i/\partial_\alpha)(\alpha^{\#}) = 0, \quad \alpha_i^{\#} = 0)$$

occurs at a wavenumber of $\alpha_r^{\#} = 0{\cdot}26763$. The dispersion relation (A 1) can be differentiated to provide series expansions for the derivatives $(\partial^n\omega/\partial\alpha^n)(\alpha^{\#})$. These were evaluated for $\alpha = \alpha^{\#}$ and are given in table 1.

The coefficients A_1, A_2, etc. that occur in the higher-order terms of the steepest-descent expansion (5) can be evaluated by the procedure set out in Morse & Feshbach (1953). Writing

$$B_n = \frac{-i}{n!}\frac{\partial^n\omega}{\partial\alpha'}(\alpha^{\#}),$$

the first three coefficients are

$$A_1 = \frac{5.3}{2^3}\frac{B_3^3}{B_2^3} - \frac{3}{2}\frac{B_4}{B_2},$$

$$A_2 = \frac{5.7.9.11}{2^7.3}\frac{B_3^4}{B_2^6} - \frac{5.7.9}{2^4}\frac{B_3^2B_4}{B_2^5} - \frac{5.7}{2^3}\frac{B_4^2}{B_2^4} + \frac{5.7}{2^2}\frac{B_3B_5}{B_2^4} - \frac{5}{2}\frac{B_6}{B_2^3},$$

$$A_3 = \frac{3.7.11.13.17}{2^{10}}\frac{B_3^6}{B_2^9} - \frac{3.7.11.13.15}{2^8}\frac{B_3^4B_4}{B_2^8} + \frac{7.9.11.13}{2^6}\frac{B_3^2B_4^2}{B_2^7} + \frac{3.7.11.13}{2^5}\frac{B_3^3B_5}{B_2^7} - \frac{3.7.11}{2^4}\frac{B_4^3}{B_2^6} - \frac{7.9.11}{2^3}\frac{B_3B_4B_5}{B_2^6} - \frac{7.9.11}{2^4}\frac{B_3^2B_4}{B_2^6} + \frac{7.9}{2^3}\frac{B_5^2}{B_2^5} + \frac{7.9}{2^2}\frac{B_4B_6}{B_2^5} + \frac{7.9}{2^2}\frac{B_3B_7}{B_2^5} - \frac{7}{2}\frac{B_8}{B_2^4}.$$

Appendix B. Expansion of steepest descent around the most-amplified ray

The leading term of the steepest-descent expansion (5) is to be compared with the other approximations in the neighbourhood of the most amplified ray ($x/t = V_g$), where $(\partial\omega_i/\partial\alpha)(\alpha^\#)$ is zero on the real α-axis. The exponential term in (5) can be expanded about this point in terms of the small parameter ϵ, where

$$\epsilon = V_g - \frac{x}{t}, \quad V_g = \frac{\partial\omega}{\partial\alpha}(\alpha^\#). \tag{B 1}$$

The exponent is

$$i\left(\alpha^* \frac{x}{t} - \omega(\alpha^*)\right)t, \tag{B 2}$$

where

$$\frac{\partial\omega}{\partial\alpha}(\alpha^*) = \frac{x}{t}. \tag{B 3}$$

$\omega(\alpha)$ and $(\partial\omega/\partial\alpha)(\alpha)$ can be expanded as a Taylor series about $\alpha^\#$,

$$\frac{\partial\omega}{\partial\alpha}(\alpha) = \frac{\partial\omega}{\partial\alpha}(\alpha^\#) + (\alpha-\alpha^\#)\frac{\partial^2\omega}{\partial\alpha^2}(\alpha^\#) + \dots, \tag{B 4}$$

and in particular, when $\alpha = \alpha^\#$, using (B 1) and (B 3) we have

$$\epsilon = (\alpha^* - \alpha^\#)\frac{\partial^2\omega}{\partial\alpha^2}(\alpha^\#) + \tfrac{1}{2}(\alpha^*-\alpha^\#)^2\frac{\partial^3\omega}{\partial\alpha^3}(\alpha^\#) + \dots. \tag{B 5}$$

Hence

$$\alpha^* = \alpha^\# + \frac{\epsilon}{\dfrac{\partial^2\omega}{\partial\alpha^2}(\alpha^\#)} - \tfrac{1}{2}\epsilon^2\frac{\partial^3\omega}{\partial\alpha^3}(\alpha^\#)\Big/\left[\frac{\partial^2\omega}{\partial\alpha^2}(\alpha^\#)\right]^3 + \dots. \tag{B 6}$$

The exponent can therefore be expressed in terms of ϵ and derivatives of ω at $a^\#$ as

$$= i\left\{(\alpha^\#(V_g+\epsilon) - \omega(\alpha^\#) + \frac{\epsilon^2}{2\dfrac{\partial^2\omega}{\partial\alpha^2}(\alpha^\#)} - \frac{\epsilon^3\dfrac{\partial^3\omega}{\partial\alpha^3}(\alpha^\#)}{6\left[\dfrac{\partial^2\omega}{\partial\alpha^2}(\alpha^\#)\right]^3} + \dots\right\}t, \tag{B 7}$$

or, in a simplified notation,

$$i\left\{(\alpha^{\#}(V_g+\epsilon)-\omega)+\frac{\epsilon^2}{2\omega''}-\frac{\epsilon^3\omega'''}{6(\omega'')^3}+\ldots\right\}t. \tag{B 8}$$

Appendix C. Real axis approximation expansion around the most-amplified ray

The exponent of the real-axis approximation is given by (14) as

$$i\left\{\alpha^+\frac{x}{t}-\omega(\alpha^+)\right\}t, \tag{C 1}$$

where α^+ is chosen so that

$$\frac{\partial\omega_r}{\partial\alpha}(\alpha^+)=\frac{x}{t}. \tag{C 2}$$

Again expanding ω in a Taylor series, we get

$$\frac{\partial\omega_r}{\partial\alpha}(\alpha^+)=\frac{\partial\omega_r}{\partial\alpha}(\alpha^{\#})+(\alpha^+-\alpha^{\#})\frac{\partial^2\omega}{\partial\alpha^2}(\alpha^{\#})+\ldots, \tag{C 3}$$

and hence

$$\alpha^+=\alpha^{\#}+\frac{\epsilon}{\omega_r''}-\tfrac{1}{2}\epsilon^2\frac{\omega_r'''}{2(\omega_r'')^3}+\ldots, \tag{C 4}$$

and the exponent becomes

$$i\left\{(\alpha^{\#}(V_g+\epsilon)-\omega)+\frac{\epsilon^2(\omega_r''-i\omega_i'')}{2(\omega_r'')^2}+\frac{\epsilon^3}{6(\omega_r'')^3}[3\omega_r'''\omega''-3\omega_r'''\omega_r''+\omega'''\omega_r'']+\ldots\right\}t, \tag{C 5}$$

where ω and all the derivatives have been evaluated at $\alpha^{\#}$.

The extended form of the RAA (15) contains an additional term

$$\left(\frac{\partial\omega_i}{\partial\alpha}(\alpha^+)\right)^2\Big/2\frac{\partial^2\omega}{\partial\alpha^2}(\alpha^+), \tag{C 6}$$

and this is equivalent to

$$\frac{\epsilon^2(\omega_i'')^2}{2\omega''(\omega_r'')^2}+\frac{\epsilon^3(\omega_i'')^2}{2(\omega_r'')^3\,\omega''}\left[-\frac{\omega'''}{\omega''}+\frac{\omega_i'''}{\omega_i''}-\frac{\omega_r'''}{\omega_r''}\right], \tag{C 7}$$

and therefore the exponent can be reduced to

$$i\left\{(\alpha^{\#}(V_g'+\epsilon)-\omega)+\frac{\epsilon^2}{2\omega''}+\frac{\epsilon^3}{2(\omega_r'')^3}\left[\left(\frac{i\omega_r'''\omega_i''}{\omega_r''}-\tfrac{1}{3}\omega'''\right)+\frac{(\omega_i'')^2}{\omega''}\left(-\frac{\omega'''}{\omega''}+\frac{\omega_i'''}{\omega_i''}-\frac{\omega_r'''}{\omega_r''}\right)\right]+\ldots\right\}t. \tag{C 8}$$

REFERENCES

Craik, A. D. D. 1981 The development of wavepackets in unstable flows. *Proc. R. Soc. Lond.* A **373**, 457.

Gaster, M. 1968*a* The development of three-dimensional wave packets in a boundary layer. *J. Fluid Mech.* **32**, 173.

Gaster, M. 1968*b* Growth of disturbances in both space and time. *Phys. Fluids* **11**, 723.

Gaster, M. 1978*a* Series representation of the eigenvalues of the Orr–Sommerfeld equation. *J. Comp. Phys.* **29**, 143.

GASTER, M. 1978*b* On the application of ray mathematics to non-conservative systems. Geo Fluid Dynamical Wave Mathematics, Applied Mathematics Group, University of Washington, Seattle, Washington (1977), p. 61.

GASTER, M. 1981 The propagation of linear wave packets in laminar boundary layers. *A.I.A.A.J.* **19**, 419.

LANDAHL, M. T. 1972 Wave mechanics of breakdown. *J. Fluid Mech.* **56**, 775.

MORSE, P. M. & FESHBACH, H. 1953 *Methods of Theoretical Physics*. McGraw-Hill.

STEWARTSON, K. 1973 Some aspects of non-linear stability theory. Survey Lecture, XIth Symp. on Advanced Problems and Methods in Fluid Mechanics, Polish Academy of Sciences.